Silicon Nitride Biaxial Pointing Mirrors with Stiffening Ribs

Todd J. Kaiser, B. Jeffrey Lutzenberger, Robert A. Friholm, Phillip A. Himmer,
David L. Dickensheets

Department of Electrical and Computer Engineering
Montana State University, Bozeman MT 59717

Abstract

Gold-coated silicon nitride mirrors designed for two orthogonal rotations were fabricated. The devices were patterned out of nitride using surface micromachining techniques, and then released by a sacrificial oxide etch and bulk etching the silicon substrate. Vertical nitride ribs were used to stiffen the members and reduce the curvature of the mirrored surfaces due to internal stress in the nitride and the metal layer. This was accomplished by initially etching the silicon substrate to form a mold that was filled with nitride to create a stiffening lattice-work to support the mirrored section. Mirror diameters ranging from 100 μm to 500 μm have been fabricated, with electrostatic actuation used to achieve over four degrees of tilt for each axis.

Keywords: Biaxial mirrors, MEMS, MOEMS, stiffening ribs

1. Introduction

The Internet, cable television and teleconferencing has highlighted the increased requirement for communication bandwidth. The use of dense wavelength division multiplexing (DWDM) has increased the number of wavelengths carried on each optical fiber used to meet these high bandwidth requirements. These multiple wavelengths must be switched and rerouted to different fibers. The current method of converting the optical signal at each wavelength to slower electrical signals, switching, then converting back to optical signals and transmitting back down an optical fiber has become the dominant power and space consumer of fiber communication systems. All-optical switching methods will be developed to meet the demand for increased communication bandwidth.

Micromechanical mirror systems are one method to obtain all-optical switching. The small nature of an optical fiber makes the beam compatible with micromechanical mirrors. Movable micromechanical mirrors can be used to redirect the optical beam between fibers. This presents significant problems for the design of micromechanical mirrors.

An ideal mirror would have an optically flat surface so that the reflected beam is not significantly deformed. This will aid in the coupling efficiency into the optical fiber. It should also have a large dynamic range. The greater the tilt angle of the mirror, the more fibers can be used in the optical cross connect reducing the total number of cross connects required. The mirror should be easily produced. Complex and exotic processes increase the production costs and reduce the yield, raising the ultimate cost of the cross connect. This research is an attempt to address these issues.

Numerous authors have reported on torsional mirrors. Mirrors have used magnetics and electrostatics for actuation and have been produced using a variety of fabrication techniques[1-4]. Bulk micromachining has produced flat silicon mirrors with large deflection angles, but uses complicated processing techniques, layer bonding or expensive substrate wafers[5,6]. Surface micromachining techniques have generated mirrors with small angular deflection with small actuation voltages, but were pliable and were subject to deformation upon actuation. Creating standoffs to raise the mirror above the surface can increase the angle of deflection for surface micromachined mirrors, but this adds complexity to the fabrication

MOEMS and Miniaturized Systems II, M. Edward Motamedi, Rolf Göring, Editors,
Proceedings of SPIE Vol. 4561 (2001) © 2001 SPIE · 0277-786X/01/$15.00

process[7]. The surface micromachined structure can be stiffened by adding topology to the substrate that create stiffening beams and ribs in the deposited material. These are used to add structural integrity to the mechanical members[8,9].

A combination of the two techniques, bulk and surface micromachining can produce structures that can be made stiffer and have larger angular deflections, yet are easily produced. The mechanical members and mirror surface are made using standard surface micromachining techniques with structures to add rigidity to the members then released using a wet bulk etch of silicon.

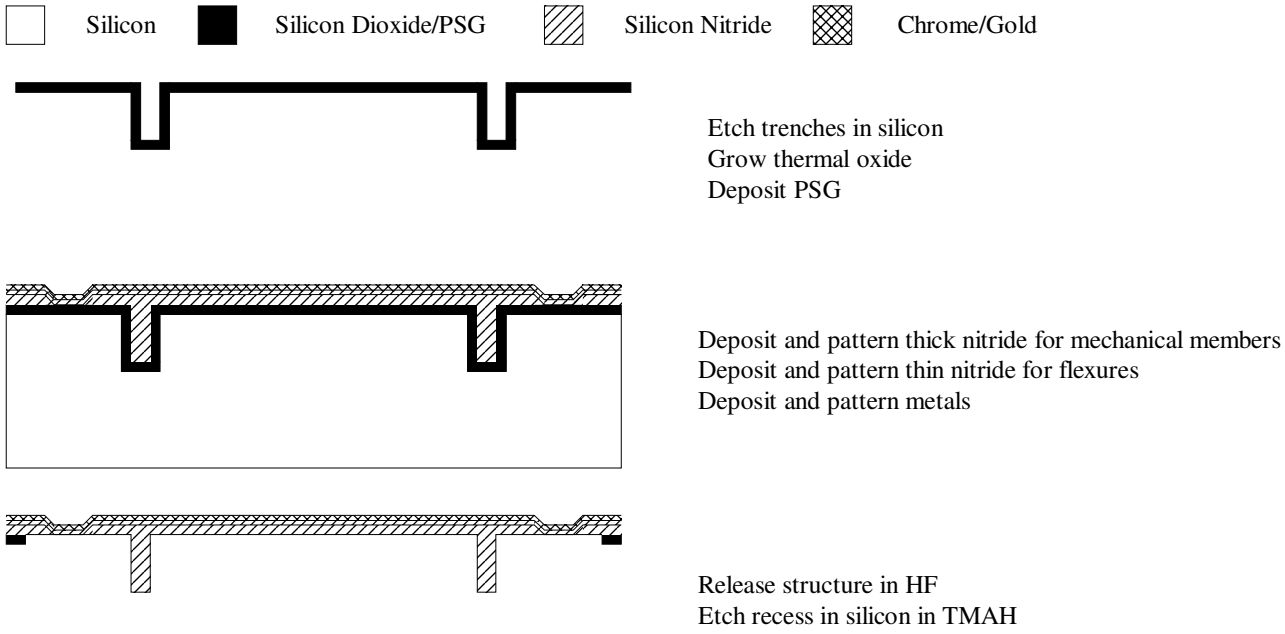

Figure 1. Process flow for fabrication of silicon nitride biaxial mirrors.

2. Fabrication

The fabrication flow is a modification of the process used to produce silicon nitride deformable membranes previously reported[10]. Instead of using the backfilling of deep reactive ion etched silicon trenches for an etch stop, the backfilled trenches become part of the structural members. Figure 1 shows an abbreviated process flow. The silicon substrate is first patterned for the stiffening lattice. The pattern is etched into the silicon using standard deep reactive ion etching (DRIE) techniques with short iteration times to minimize the typical scalloping of the sidewalls[11]. Once the trenches have been etched into the silicon, thermally grown oxide conformally coats the surface. Phosphosilicate glass (PSG) is then deposited to form a sacrificial layer between the substrate and the structural silicon nitride. The structural members are formed out of two layers of silicon nitride. The first layer backfills the etched trenches and forms the mechanical members when it is patterned and appropriately etched. The second nitride layer, usually a thinner layer, defines the flexures. This allows for an increased design space, with the flexure thickness being the additional design variable. Chrome-gold is deposited and patterned to form the reflective surface, the electrodes, interconnects and bonding pads. Actuation electrodes are positioned on the outer member to deflect the structure about the axis defined by the outer flexures and on the inner electrodes to deflect the structure about the axis defined by the inner flexures. Actuation is made by applying a potential between the substrate and the electrodes on the surface of the device.

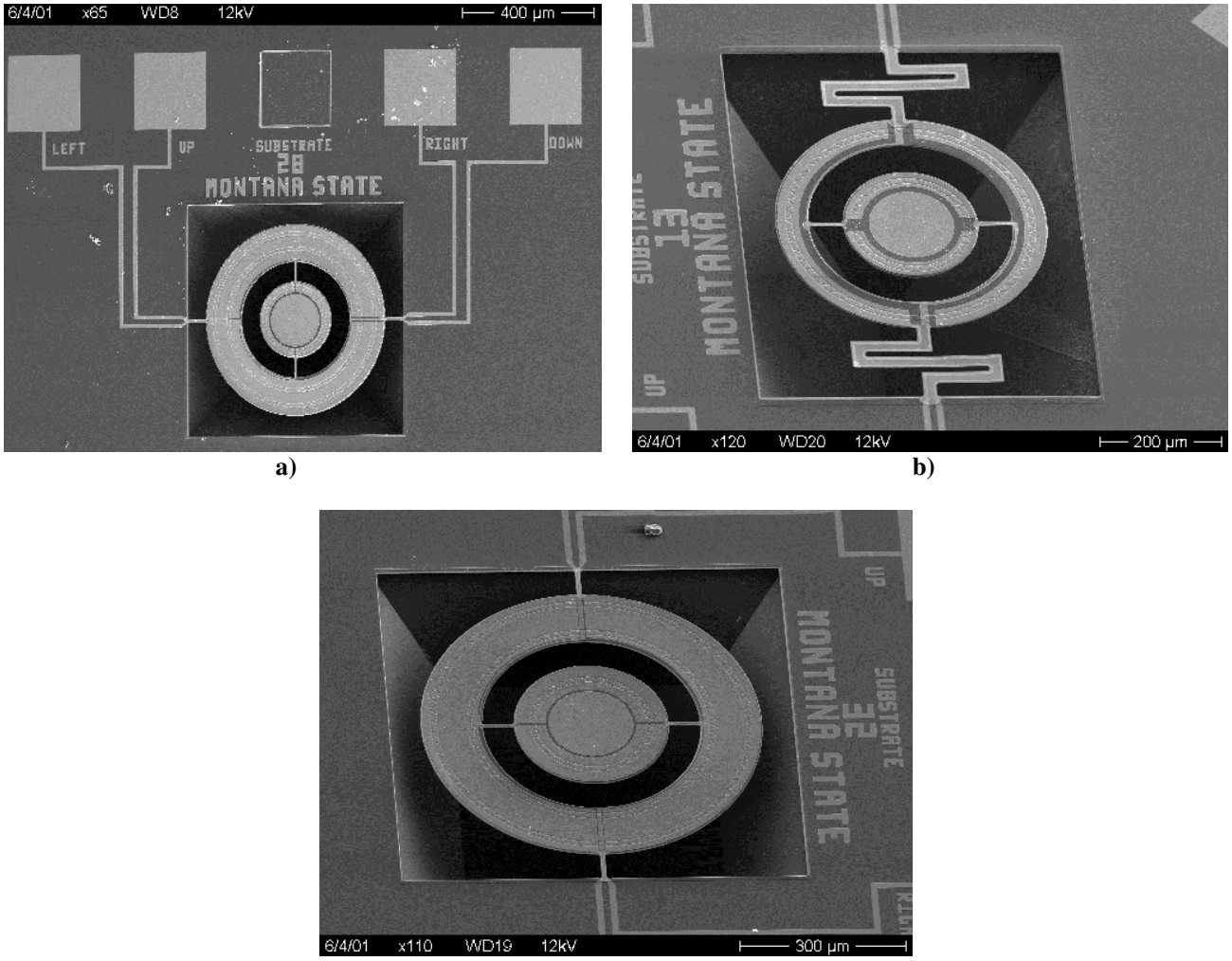

Figure 2. Scanning electron microscope images of released biaxial mirrors.

The devices are released by etching the sacrificial PSG and thermal oxide with a hydrofluoric acid (HF) solution. The clearance for mechanical motion is then produced by anisotropic etching the silicon substrate in a tetramethyl ammonium hydroxide solution ($(CH_3)_4NOH$, TMAH). Various concentrations and etch temperatures were used. A 5% solution of TMAH at 80 ºC produced an etch rate of 25 µm/hr under the silicon nitride with the stiffening ribs. The silicon etch in TMAH was timed to produced the desired recess under the biaxial mirrors.

Various fabricated and released devices are shown in Figure 2. Thirty-two different biaxial mirror designs and numerous test structures are produced on a die with 34 die on a four-inch wafer. The biaxial mirrors had a range of flexure geometries and dimensions, stiffening members, actuator sizes and reflective surface dimensions. Different geometries for the flexures included meander hinges (Figure 2b), recessed hinges and standard torsional hinges (Figure 2a & 2c).

Figure 2c shows a typical device. It has a reflective surface with a 150 µm diameter. The inner actuator is 50 microns wide and the outer electrode is 100 microns wide. The flexures are all 50 µm long with the inner width being 6 µm and

the outer flexure width being 8 microns. It has two individual stiffening rings with webbing on the outer member and one webbed stiffening ring on the inner member.

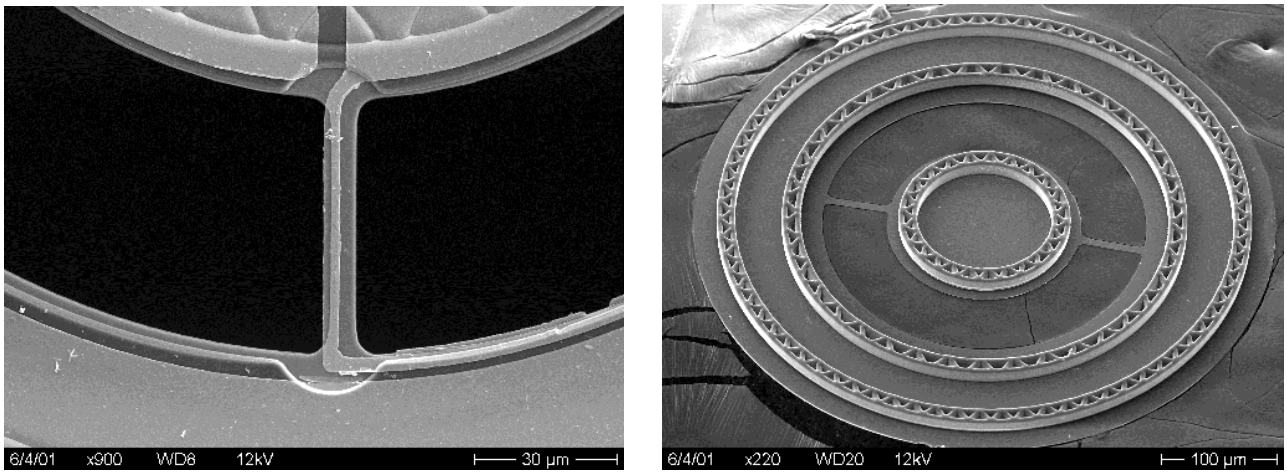

Figure 3. Enlarged view of detail features on biaxial mirrors. Front side of close up on the inner flexure with two layers of nitride (a). Backside of biaxial mirror with stiffening ribs visible. (b)

The details of an inner flexure can be seen in Figure 3a. The step down between the two layers of nitride can be seen as arcs at the end of the flexures. Also visible are the undulations over the backfilled trenches near the top of the image. The cusps over the backfilled trenches create a surface unsuitable for a reflective mirror, therefore no trenches were incorporated in the mirror area. Figure 3b shows the backside of a biaxial mirror. The backfilled trenches that increase the structural strength of the device can be seen. The height of the lattice-work is determine by the etch depth into the silicon substrate, typically 10-15 microns. Various geometries of lattice-work were produced ranging from simple concentric rings to interlaced webbings that completely filled the dimensions of the structure.

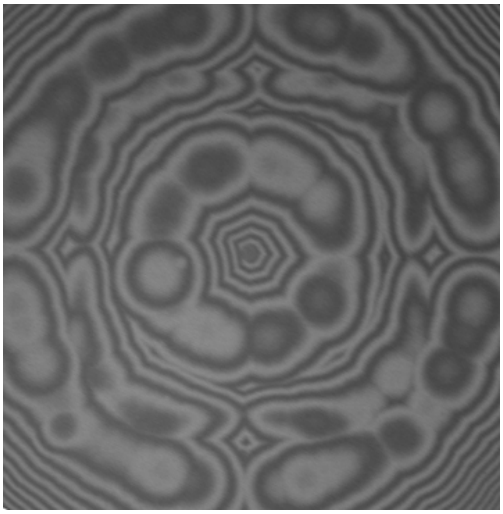

Figure 4. Interferometric image of substrate silicon with mirror removed.

A mirror structure was removed from one of the devices to visually inspect the substrate silicon under the released biaxial mirror. It was then placed in an interference microscope with a 660nm source. Figure 4 shows the resulting image of the substrate under the removed biaxial mirror. Each fringe represents a half wavelength difference in vertical height, approximately a third of a micron. The bubble-like regions in the image correspond to where the stiffening members were etched into the silicon and are at a lower elevation. The substrate under the mirror is flat to within a few microns.

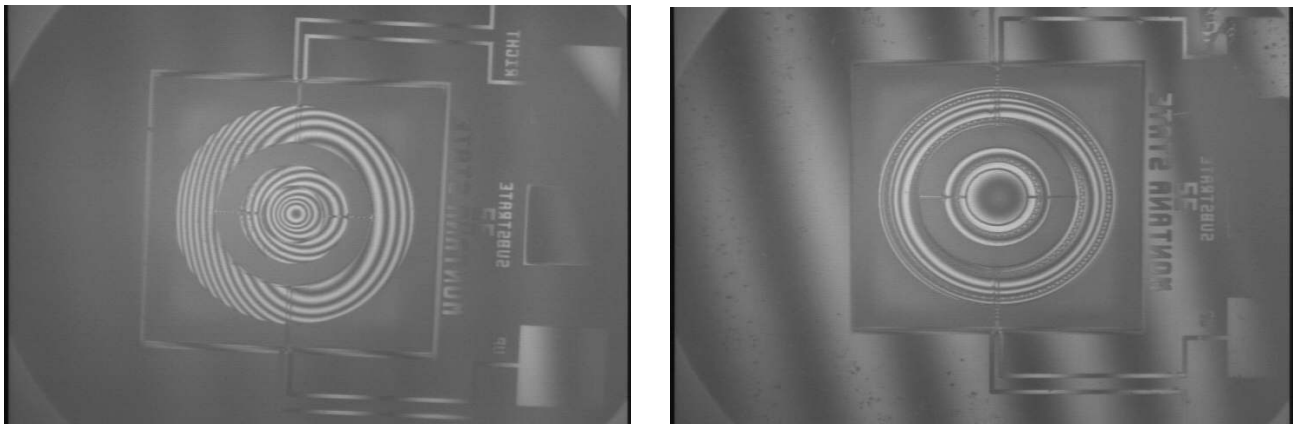

a) **b)**

Figure 5. Comparison of flatness of structures without (a) and with stiffening features (b). The mirror diameter is 150 microns.

3. Results

Several of the die on the substrate wafer are produced without first etching the silicon surface. These die will not have the stiffening ribs. This allows for a direct comparison of identical devices from the same wafer that have the stiffening members and those without the stiffening structures. Figure 5 shows a result of that comparison. The image on the left (Figure 5a) has no stiffening ribs. The deformation of the device can be seen by the numerous fringes throughout the device compared to the few straight fringes on the substrate. The image on the right (Figure 5b) has the stiffening rings and demonstrates a great reduction in fringes. The device still has some curvature that can be seen as the concentric fringes on the device when compared to the straight fringes seen on the flat substrate.
The reflective portion of the device is 150 microns in diameter and has less than one fringe across it. The source of the curvature is stress induced on the loss stress nitride by the chrome-gold metal layers. Typically, the nitride has stress levels of 50-100 MPa, and the 50Å of chrome and 1000Å of gold create additional stress in the layered film.

Electrostatic actuation of the biaxial mirror is shown in Figure 6. The first image (Figure 6a) is the static case with no applied voltages. The fringes seen are due to the combination of the surface deformation and substrate tilt, which is visible at the top of the image. It is apparent that there is some curvature on the outer member demonstrated by the nonlinear fringe pattern, but the center mirror is relatively flat since its fringe pattern is nearly linear. The middle image (Figure 6b) has an applied potential between the substrate and the electrode on the left side of the outer member. This applied voltage creates an electrostatic torque that tilts the entire mechanical structure. Similarly, applying a voltage to the right electrode tips the mirror and the supporting outer member to the right. The adjustment of the relative potentials between the right and left electrode and the substrate has produced over plus and minus four degrees of rotational motion.

Figure 6c shows the results of applying a potential to the upper electrode. The inner support member for the mirror does tilt up as expected, but there is some movement about the orthogonal axis. This can be noted in the image by the increased number of fringes across the outer member when compared to the static case in Figure 6a. Further investigation is necessary to quantify the effect and determine if it is a symmetry issue. Initial finite element analysis has demonstrated that some off primary axis motion can be expected by the current asymmetric design. Different mirror

designs had different coupling magnitudes. Some demonstrated almost no coupling but others had significant cross axis motion.

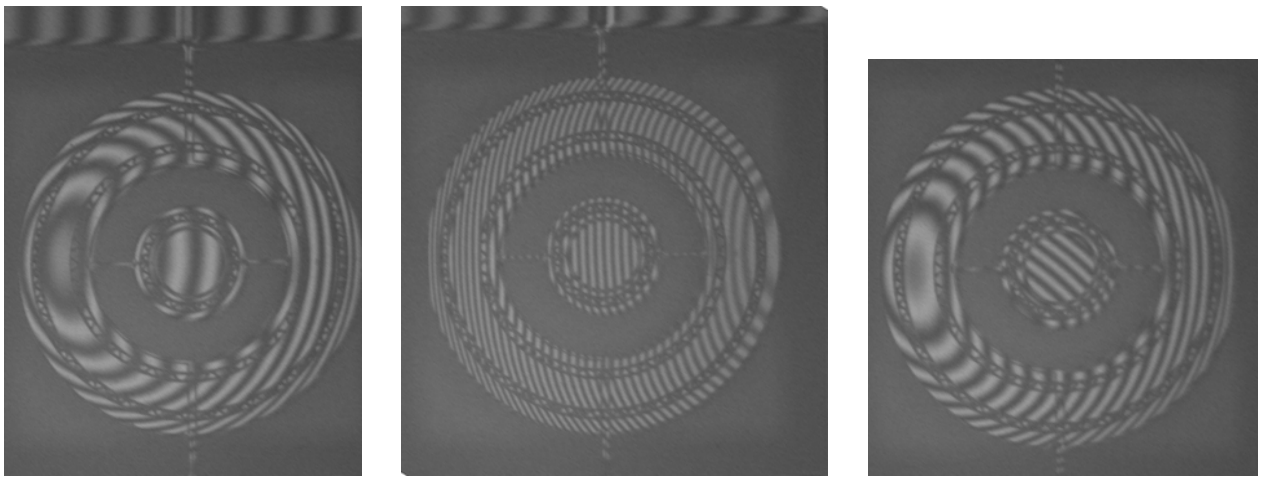

a) b) c)

Figure 6. Interferometric images of a biaxial mirror with no applied voltages (a), applied voltage to outer left electrode (b) and applied voltage to inner top electrode (c).

4. Conclusions

Micromachined biaxial mirrors were produced using a combination of bulk and surface micromachining. Deep reactive ion etching the substrate produced a trench that is back filled with surface micromachining techniques. This created a structure that was not only stiffer but also flatter than was produced by surface micromachining only. Mirrors were produced with a fraction of a micron curvature due to the stiffening of the mechanical structure. Large deflections over 4 degrees were made possible by bulk etching the substrate silicon to produce recess depths on the order of 100 microns. Future studies are planned to model and characterize the dynamical properties of the biaxial mirror.

5. Acknowledgements

The authors would like to thank Eric Perozziello for fabricating our devices and the Stanford Nanofabrication Facility for providing the fabrication facilities through the National Nanofabrication Users' Network.

References

1. K. E. Petersen, “Silicon Torsional Scanning Mirrors,” *IBM J. Res. Develop.*, **24**, pp. 631-637, 1980.

2. L. J. Hornbeck, “Deformable Mirror Spatial Light Modulators, *Proc. SPIE*, **1150**, pp. 1-17, 1989.

3. M. Fischer, H. Graef, W. von Münch, “Electrostatically Deflectable Polysilicon Torsional Mirrors,” *Sens. Actuators A*, **44**, pp. 83-89, 1994.

4. A. S. Dewa, J. W. Orcutt, M, Hudson, D. Krozier, A. Richards, H. Laor, "Development of a Silicon Two-Axis Micromirror for Optical Cross-Connect," *2000 Solid-State Sensor and Actuator Workshop*, pp 93-96, 2000.

5. D. W. Wine, M. P. Helsel, L. Jenkins, H. Urey, T. D. Osborn, "Performance of a Biaxial MEMS-Based Scanner for Microdisplay Applications," *Proc. SPIE*, **4178**, pp.186-196, 2000.
6. D. Dickensheets, G. Kino, "Microfabricated Biaxial Electrostatic Torsional Scanning Mirrors," *Proc. SPIE*, **3009**, pp. 141-150, 1997

7. V. A. Aksyuk, F. Pardo, C. A. Bolle, S. Arney, C. R. Giles, D. J. Bishop, "Lucent Microstar Micromirror Array Technology for Large Optical Crossconnects," *Proc. SPIE*, **4178**, pp. 320-324, 2000.

8. H.Y. Lin, W. Fang, "Rib-reinforced Micromachined Beam and its Applications," *J. Micromech. Microeng*., **10**, pp. 93-99, 2000.

9. J. Drake, H. Jerman, "A Micromachined Torsional Mirror for Track Following in Magneto-optical Disk Drives," *2000 Solid-State Sensor and Actuator Workshop*, pp 10-13, 2000.

10. D. L. Dickensheets, P. A. Himmer, R. A. Friholm, B. J. Lutzenberger, "Miniature High-resolution Imaging System with 3-dimensional MOEMS Beam Scanning for Mars Exploration," *Proc. SPIE*, **4178**, pp. 90-97, 2000.

11. A. A. Ayon, R. Braff, C. C. Lin, H. H. Sawin, M. A. Schmidt, "Characterization of a Time Multiplexed Inductively Coupled Plasma Etcher," *J. Electrochem. Soc.* **146**, pp.339-349, 1999.